Directional Anisotropy in the Cleavage Fracture of Silicon

Rubén Pérez [1,2] and Peter Gumbsch [2]

[1] *Departamento de Física Teórica de la Materia Condensada, Universidad Autónoma de Madrid, E-28049 Madrid, Spain*
[2] *Max Planck Institut für Metallforschung, Seestrasse 92, 70174 Stuttgart, Germany*

(Received 4 November 1999)

Total-energy pseudopotential calculations are used to study the cleavage anisotropy in silicon. It is shown that cracks propagate easily on {111} and {110} planes provided crack propagation proceeds in the $\langle \bar{1}10 \rangle$ direction. In contrast, if the crack is driven in a $\langle 001 \rangle$ direction on a {110} plane the bond breaking process is discontinuous and associated with pronounced relaxations of the surrounding atoms, which results in a large lattice trapping. The different lattice trapping for different crack propagation directions can explain the experimentally observed cleavage anisotropy in silicon single crystals.

PACS numbers: 62.20.Mk, 71.15.Nc

The catastrophic failure of materials is ultimately determined by events on the atomic scale. This is particularly clear in the case of brittle fracture, where the crack at its tip must be atomically sharp and move by breaking individual bonds between atoms. Such a brittle crack can therefore be regarded as a probe for the atomic bonding.

Semiconductors and particularly silicon are materials that may be suitable to test the perfectly brittle case experimentally. Silicon can be produced as a virtually dislocation-free single crystal and crack tips have been observed in the transmission electron microscope to propagate in the absence of dislocations [1]. Silicon has been studied extensively for its fracture characteristics [2–4]. In short, silicon is reported to have two principal cleavage planes: {111} planes, usually the easy cleavage plane [5], and {110} planes [4], the planes of easy cleavage in polar III-V semiconductors [6]. Different crack propagation directions have been studied for both crack planes. The $\langle 110 \rangle$ propagation direction was seen to be the preferred propagation direction on both cleavage planes [4,5]. On the {111} fracture surface an anisotropy with respect to propagation direction manifests itself only in faint markings along $\langle 110 \rangle$ directions. In contrast, cleavage fracture on the {110} plane is very anisotropic as shown schematically in Fig. 1. Propagation along the $\langle 110 \rangle$ direction is easy and results in nearly perfectly flat fracture surfaces, while propagation along the $\langle 111 \rangle$ direction is difficult to achieve and never gives flat fracture surfaces [5]. Attempts to achieve propagation in the $\langle 001 \rangle$ direction, perpendicular to the preferred direction have not been successful [7,8] because the crack deflects onto {111} or {112} planes [8], as shown in Fig. 2 [8].

An anisotropy with respect to crack propagation direction is difficult to understand theoretically. Following Griffith [9] one may regard the static brittle crack as a reversible thermodynamic system for which one seeks equilibrium. In equilibrium, the mechanical energy release upon crack advance $\mathcal{G}$ must be in balance with the energy required to create the two new surfaces 2γ. The Griffith criterion, $\mathcal{G} = 2\gamma$, is not really a fracture criterion but only a necessary condition for fracture. Nevertheless, the Griffith criterion leads to two important conclusions: (1) crystal lattice planes with low surface energies are energetically favored as cleavage planes and (2) independent of the propagation direction, a given cleavage plane will have a single unique value of $\mathcal{G}$. A perfectly brittle crack in a crystal is therefore expected to choose a cleavage plane with low surface energy and to propagate on this plane with equal ease in all directions.

From an atomistic point of view the situation is somewhat different. The first atomistic studies of fracture showed that the discreteness of the lattice manifests itself in the so-called lattice trapping effect [10,11]. Lattice trapping causes the crack to remain stable and not to advance until loads somewhat larger than the Griffith load are reached. It has been shown that the magnitude of the trapping range strongly changes with the bonding characteristics [11–13]. Lattice trapping may also depend on the direction in which the crack tip bonds are broken and may therefore be different for crack propagation along different crystallographic directions on one cleavage plane [14,15].

Atomistic modeling of cracks is a rather complicated problem because both the long-range elastic interactions and the short-range chemical interactions are needed for a correct description of the problem. This either requires a large atomistic model or one has to embed the atomistic region into a flexible surrounding [14,16]. Therefore, crack propagation has previously been studied mainly by

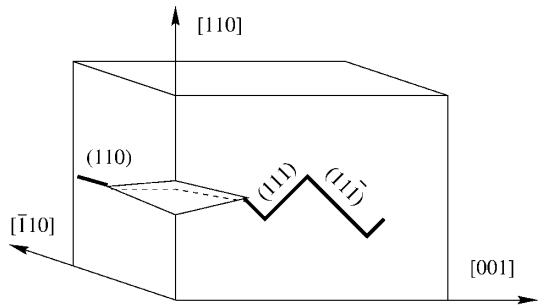

FIG. 1. Schematic drawing of the experimentally observed crack propagation modes along different crystallographic directions on the (110) plane.

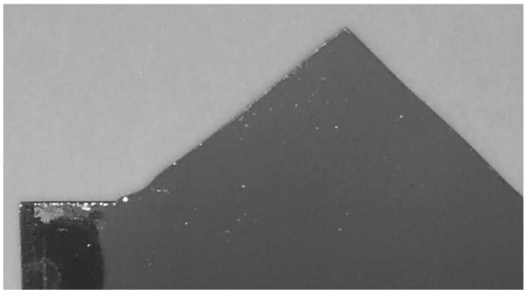

FIG. 2. Side view (lateral width is 25 mm) of a $\{\bar{1}10\}$ wafer broken in uniaxial tension along a $\langle 110\rangle$ direction. The crack propagates on planes inclined by 35° and more with respect to the macroscopic $\{110\}$ crack plane. Figure courtesy of T. Cramer [8].

simple empirical interaction models. A recent study on silicon [17] clearly demonstrated the limits of these empirical descriptions for the application in fracture simulations. To obtain crack propagation it was necessary to manipulate the three-body term of the Stillinger-Weber potential [18], which then of course introduced unwanted changes to the bulk properties. We have experienced similar problems in our attempt to simulate crack propagation in silicon with the Tersoff potential [19]. Despite the fact that this potential is able to describe the surfaces quite nicely [19], our simulations showed unphysical structural transitions at the crack tip. The purpose of this paper is to atomistically analyze the stability of brittle cracks in silicon single crystals. The analysis is based on a full quantum mechanical study of the bond breaking process, where particular attention is paid to the anisotropy with respect to the crack propagation direction and to effects of the system size. It will be shown that some of the important atomistic effects can even be seen in very small models.

The energies and atomic forces are calculated within density functional theory in the local density approximation in its plane wave pseudopotential formulation [20]. An optimized nonlocal pseudopotential [21] is used for silicon. The optimization makes the pseudopotential rapidly convergent with the cutoff energy of the plane wave expansion [22]. A bare Coulomb potential is used for the hydrogen atoms which saturate the dangling bonds at the outer surface of the atomistic model.

Cracks on the $\{110\}$ plane with $\langle 001\rangle$ and $\langle 1\bar{1}0\rangle$ crack fronts (shown in Fig. 3) and a $\{111\}$ crack with a $\langle 0\bar{1}1\rangle$ crack front are considered. Periodic boundary conditions are applied along the crack front direction to simulate plane strain conditions. The elastic field of the crack is applied to the atomistic region by means of displacement boundary conditions. The outermost two layers of silicon atoms (see Fig. 3) are held fixed at the positions given by the anisotropic linear elastic solution for a straight crack under opening mode loading [23], while the other atoms are relaxed using a conjugate gradient method.

The magnitude of the loading is characterized by the stress intensity factor K. The energy release rate can directly be obtained from the square of the stress intensity

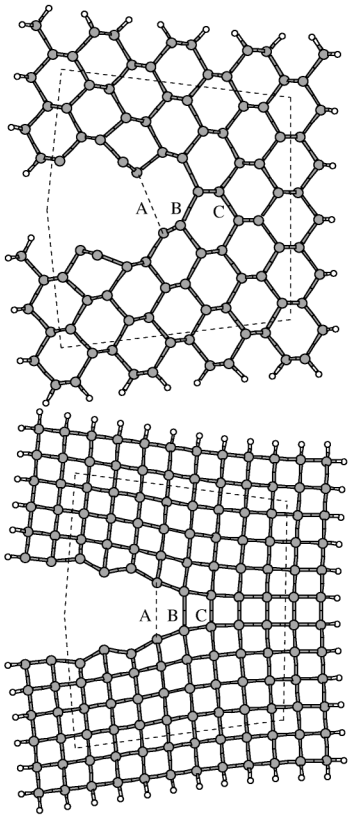

FIG. 3. Relaxed atomic configuration for the $(110)[\bar{1}10]$ (above) and the $(100)[001]$ (below) crack orientations at a load of $K_I = 1.20K_I^G$. The atoms outside the dashed line are kept fixed at the positions given by the elastic solution during the relaxation process.

factor with a constant conversion factor [23], which is given in Table I together with the system sizes, the surface energies, and other relevant information on the different crack systems.

The calculations are started at a stress intensity K_G which fulfills the Griffith criterion. All crack systems are stable at this load, which means that the crack tip does not advance or recede during relaxation. The relaxed structures are then taken as the starting point for further loading or unloading by proportional scaling of all displacements and subsequent relaxation. Loading or unloading is performed in increments of 5% of the Griffith load.

The fracture toughness is determined from the critical load K^+ at which the crack tip bond breaks and the crack advances upon increasing the load. Similarly a critical load for crack closure K^- can be determined upon decreasing the load. The lattice trapping regime, where the crack remains at one particular position in the lattice, is given by $\Delta K = K^+/K^- - 1$.

The breaking of the crack tip bond can be determined by monitoring the bond distances across the crack plane. Figure 4 shows the bond distances of the bonds close to the crack tip of the two $\{110\}$ crack systems as a function of the applied load. Two different system sizes are shown on the same plot. The labeling of the bonds corresponds

TABLE I. Dimensions and crystallography of the crack systems considered. The dimensions are given in units of the bulk lattice parameter of the 8-atom cubic unit cell of silicon. The surface energies (γ) are calculated for the relaxed buckled (110) surface and the 2×1 Pandey reconstruction of the (111) surface. The values for $K^2/\mathcal{G}$ are calculated from the experimental elastic constants [24].

Crack orient (plane) [front]	Dimensions	No. of atoms Si + H	γ J/m^2	$K^2/\mathcal{G}$ GPa
(110) $[1\bar{1}0]$	$\frac{7}{2} \times \frac{5}{2}\sqrt{2} \times \frac{\sqrt{2}}{2}$	68 + 34	1.73	57.8
Large	$\frac{8}{2} \times \frac{6}{2}\sqrt{2} \times \frac{\sqrt{2}}{2}$	96 + 42	...	...
(110) [001]	$2\sqrt{2} \times 2\sqrt{2} \times 1$	64 + 32	1.73	52.1
Large	$3\sqrt{2} \times 3\sqrt{2} \times 1$	144 + 48	...	...
(111) $[0\bar{1}1]$	$\frac{3}{2}\sqrt{6} \times 2\sqrt{3} \times \sqrt{2}$	70 + 26	1.44	56.2

to Fig. 3. It is apparent that bond A is broken and bond B is intact at the lowest displayed loads.

Upon loading the (110) $[1\bar{1}0]$ crack system, the bond length of bond B increases gradually up to a load below $K^+ = 1.35K_G$, at which the bond length increases significantly. This sudden increase in bond length from about 3 Å to about 4 Å is a clear signature of the bond breaking process. The bond breaking occurs at the same load for both system sizes. However, the jump in bond length and the corresponding structural relaxations of the surrounding atoms are significantly more pronounced for the larger system. Similarly bond A is healing upon unloading at a load of $K^- = 0.85K_G$ (not shown in Fig. 4) so that the (110) $[1\bar{1}0]$ crack system is characterized by a lattice trapping range of $\Delta K = 0.6$.

Neither the (110) [001] crack system (shown in Fig. 4) nor the (111) $[01\bar{1}]$ crack system show such an abrupt bond breaking process. The crack tip bonds appear to continuously lengthen from 3 to 4 Å upon loading. Similarly, the bonds close continuously upon unloading. This makes it difficult to precisely determine the upper and lower critical loads but has no effect on the magnitude of the trapping range. If a bond length of 3.3 Å is taken as the critical distance, the (110) [001] crack system gives $K^+ = 1.25K_G$ and $K^- = 0.95K_G$. The lattice trapping range is $\Delta K = 0.3$. This trapping range decreased by 0.05 upon increase of the system size from the smaller to the larger system. Furthermore, it is interesting to note that the crack propagates further and even breaks bond C upon increasing the load to $1.4K_G$ in the large system.

The (111) $[01\bar{1}]$ crack system gives the same lattice trapping range and critical loads ($K^{\pm} = 0.95 - 1.25K_G$) as the (110) [001] crack system with similar difficulties in the definition of precise upper and lower critical loads.

The calculations for the (111) $[01\bar{1}]$ crack system can be compared to previous studies [25], which used a non-self-consistent *ab initio* tight-binding scheme and an extrapolation method to determine the lattice trapping range. A lattice trapping range of $\Delta K = 0.3$ is reported for the largest model, which is in good agreement with our result despite the very different methods used.

Two distinct types of bond breaking processes are observed here: A continuous process without pronounced structural relaxations and a clearly discontinuous abrupt bond breaking event. The continuous process mimics what one would expect from continuum theory and therefore results only in a relatively narrow lattice trapping range. The magnitude of the trapping range decreases upon increasing the system size. Consequently, the trapping in the continuous process may partly be regarded as an effect of the limited system size. One may then conjecture that the trapping range could decrease further upon increasing the system size to macroscopic dimensions. In either case, the low lattice trapping leads to easy propagation of cracks in directions in which a continuous bond breaking occurs. In contrast, the discontinuous process is clearly connected to structural rearrangements at the crack tip. Comparing the different system sizes, it is apparent that the lattice trapping is mainly a result of the relaxations of the 6 or 8 atoms immediately surrounding the crack tip. The magnitude of the trapping range therefore does not change with system size even for very small systems. Atomic rearrangements and relaxations in the immediate neighborhood of the crack tip can therefore be made responsible for the large trapping range.

A small lattice trapping range should lead to low fracture toughness and easy propagation of cracks in the $\langle 110 \rangle$ direction in which a continuous bond breaking occurs. In contrast, the discontinuous process which is connected to large lattice trapping should result in a higher fracture toughness. Consequently, the calculations give a very pronounced anisotropy with respect to crack propagation in different directions on the silicon (110) plane.

Comparing the calculated propagation anisotropy for $\{110\}$ cleavage to fracture experiments [5,7,8] it seems as if the agreement is only qualitative. Propagation in the "difficult" $\langle 001 \rangle$ direction is not seen in experiments, which instead show a deviation of the crack from the original plane onto inclined planes, while crack propagation continues on the $\{110\}$ plane in the simulations. To assess the possibility for the crack to deviate from the original (110) plane, one can compare the opening stress intensity on the (111) plane inclined by $\Theta = 35.3°$ with respect to the (110) $[\bar{1}10]$ crack with the fracture toughness of the (111) $[\bar{1}10]$ crack system. The inclination of course decreases the opening stress intensity compared to the

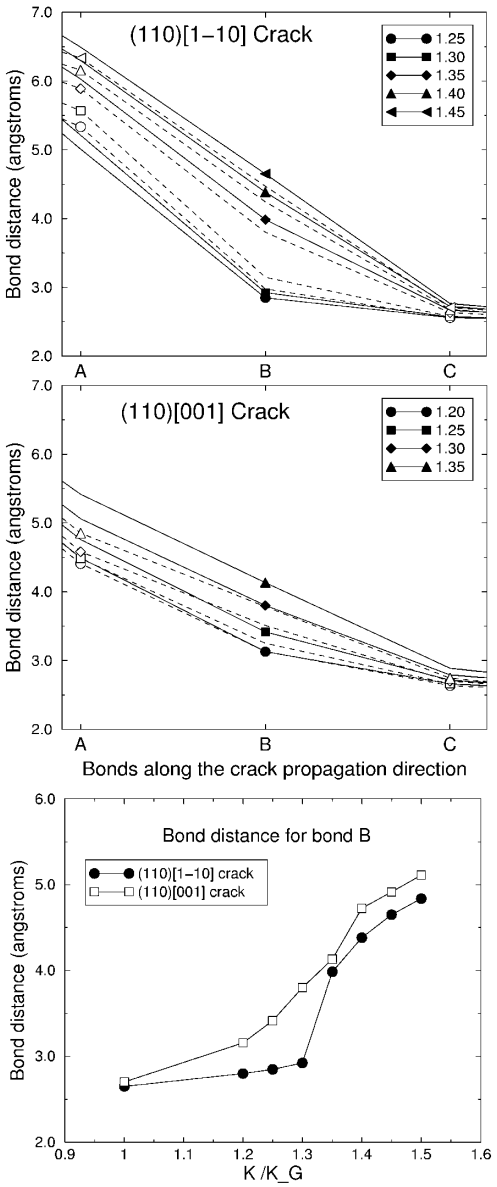

FIG. 4. Comparison of the bond distances (in Å) as a function of the stress intensity factor for the medium (dashed lines and empty symbols) and large (continuous lines and filled symbols) systems with the $(110)[\bar{1}10]$ (top) and the $(110)[001]$ (center) orientations. Bottom: Bond distance for bond B as a function of the stress intensity for the two crack orientations. The two different types of bond breaking processes can be clearly seen. Notice that the additional jump at $1.4K_G$ for the $(110)[001]$ crack is due to the breaking of bond C.

opening stress intensity on the original (110) plane. However, the large lattice trapping in the "difficult" $(110)[\bar{1}10]$ crack system just compensates this decrease. At the upper lattice trapping limit of the $(110)[\bar{1}10]$ crack system the opening stress intensity on the inclined (111) plane is $K_{\Theta\Theta}(35.3^\circ) = 1.03K_{(111)[\bar{1}10]}$. The finding that the crack did not deviate, although in principle it could, most certainly has to be attributed to the small size of the system, which stabilizes the crack on the original plane to which the boundary conditions apply.

The inclined crack of course also experiences a mixed mode (opening and shear) loading, which actually exerts a higher driving force on the crack than just the opening component. However, the influence of the mode mixity on the lattice trapping is completely unknown until today and must be deferred to future investigations, which probably require larger system sizes as well.

One of the important side aspects of the present calculations is that the *ab initio* calculations presented here provide the basis for the development of future improved empirical potentials for silicon. The results of the crack tip calculations probe the atomic bonding during the breaking process in a range of distances which is hardly accessible to other calculations and which is of crucial importance if an improved potential is to be used in mechanically distorted environments.

R. P. acknowledges the financial support from the CI-CyT (Spain) under Project No. PB97-0028.

[1] D. Clarke, in *Semiconductors and Semimetals* (Academic Press, New York, 1992), Vol. 37, pp. 79–142.
[2] C. F. St. John, Philos. Mag. **32**, 1193 (1975).
[3] M. Brede and P. Haasen, Acta Metall. **36**, 2003 (1988).
[4] G. Michot, Cryst. Prop. Prep. **17&18**, 55–98 (1988).
[5] A. George and G. Michot, Mater. Sci. Eng. A **164**, 118 (1993).
[6] R. W. Margevicius and P. Gumbsch, Philos. Mag. A **78**, 567 (1998).
[7] G. Michot (private communication).
[8] T. Cramer (unpublished).
[9] A. A. Griffith, Philos. Trans. R. Soc. London A **221**, 163 (1921).
[10] R. Thomson, C. Hsieh, and V. Rana, J. Appl. Phys. **42**, 3154 (1971).
[11] J. E. Sinclair and B. R. Lawn, Proc. R. Soc. London A **329**, 83 (1972).
[12] J. E. Sinclair, Philos. Mag. **31**, 647 (1975).
[13] W. A. Curtin, J. Mater. Res. **5**, 1549 (1990).
[14] S. Kohlhoff, P. Gumbsch, and H. F. Fischmeister, Philos. Mag. A **64**, 851 (1991).
[15] J. Riedle, P. Gumbsch, and H. F. Fischmeister, Phys. Rev. Lett. **76**, 3594 (1996).
[16] M. Ortiz and R. Phillips, Adv. Appl. Mech. **36**, 1 (1999).
[17] D. Holland and M. Marder, Phys. Rev. Lett. **80**, 746 (1998).
[18] F. H. Stillinger and T. A. Weber, Phys. Rev. B **31**, 5262 (1985).
[19] J. Tersoff, Phys. Rev. B **38**, 9902 (1988).
[20] M. C. Payne *et al.*, Rev. Mod. Phys. **64**, 1045 (1992).
[21] J. S. Lin, A. Qteish, M. C. Payne, and V. Heine, Phys. Rev. B **47**, 4174 (1993).
[22] R. Pérez, I. Stich, M. C. Payne, and K. Terakura, Phys. Rev. B **58**, 10 835 (1998).
[23] G. C. Sih and H. Liebowitz, in *Fracture*, edited by H. Liebowitz (Academic Press, New York, 1968), pp.67–190.
[24] J. P. Hirth and J. Lothe, *Theory of Dislocations* (John Wiley & Sons, New York, 1982), 2nd ed.
[25] J. C. H. Spence, Y. M. Huang, and O. Sankey, Acta Metall. Mater. **41**, 2815 (1993).